DOI: 10.1002/ejic.200500833

DFT Calculations of the ^{183}W NMR Chemical Shifts in Reduced Polyoxotungstates

Jose Gracia,[a] Josep M. Poblet,*[a] Jorge A. Fernández,[a] Jochen Autschbach,[c] and Leonid P. Kazansky*[b]

Keywords: Density-functional calculations / NMR spectroscopy / Tungsten / Oxygen / Polyoxometalates

A relativistic DFT method (ZORA) is used to calculate the ^{183}W and ^{17}O NMR chemical shifts for the reduced polyoxotungstates $W_5O_{18}W^{II}NO^{3-}$, γ-$SiW_{12}O_{40}^{6-}$, $P_2W_{18}O_{62}^{8-}$, and $W_{10}O_{32}^{6-}$ with different degrees of (de)localization of the electrons introduced. Despite some discrepancies in the calculated and experimental data, the calculations adequately describe the changes in the chemical shifts upon reduction. The reduction of a fully oxidized anion is accompanied by an expansion of the geometry. The effect of the charge localization and change in geometry on the chemical shift is evaluated. The shift of the resonance of the tungsten atoms largely depends on the reduced charge acquired upon reduction. On the other hand, those tungsten atoms that do not increase the electron density upon reduction have a negative shift. The calculations also reproduce the negative shifts of all the ^{17}O NMR resonances upon reduction of the polyoxotungstates.

Introduction

Because of the well-known ability of polyoxometalates (POM) consisting of V^V, Mo^{VI}, and W^{IV} to be reversibly reduced by one, two, or more electrons, they have attracted much attention in catalysis and other fields where redox reactions are quite important.[1–4] Depending on the molecular structure, electrons delocalize over the whole of the coordination sphere or just a part of it. EPR[1,5,6] and, subsequently, ^{17}O NMR spectroscopy[7] have proved that a single electron can be delocalized and that this delocalization can be "frozen out" at quite low temperatures (several degrees kelvin).

The second electron introduced by a certain mechanism generally pairs with the first one. ^{17}O NMR[7,8] and then ^{183}W NMR[9–11] spectroscopy have shown that the electron pair formed is completely delocalized in the Keggin anion $SiW_{12}O_{40}^{6-}$, partly in the Dawson anion $P_2W_{18}O_{62}^{8-}$, in $W_{10}O_{32}^{6-}$ or γ-$SiW_{12}O_{40}^{6-}$, and resides completely on specific atoms in γ-$SiW_{10}W^V_2S_2O_{38}^{6-}$,[12] γ-$SiMo^V_2W_{10}O_{40}^{6-}$,[10] and $P_2W_{15}Mo_3O_{62}^{8-}$ (delocalization of the electron pair over three Mo atoms),[13] or, in the case of six electrons, in $XW_9W_3^{IV}O_{40}H_6^{x-}$ (localization of six electrons in triplet forming metal–metal bonding).[14,15] In some specific cases, the introduction of two electrons entails the localization of one electron on one atom while the second electron partially delocalizes over the tungsten atoms adjacent to the first reduced atom (for example $P_2W_{17}Mo^VO_{62}^{8-}$).[13]

Several cases, however, should be considered separately. In the nitrosyl complexes $W_5O_{18}W^{II}NO^{3-}$ with the Lindqvist-type structure,[16] $PW_{11}W^{II}NO_{40}^{8-}$, and the corresponding Ru complexes with the Keggin structure,[17–19] the electron density of the cation introduced delocalizes onto the neighboring tungsten atoms.

In all the examples mentioned above, the degree of delocalization was monitored by NMR spectroscopy and estimated by the characteristic positive shift of the resonance lines attributed to the tungstens accepting the electron density. At the same time, some resonances undergo negative shift which, depending on the structure and position of the most important atom in it, may be rather significant.

In this paper we report DFT calculations of the ^{183}W and ^{17}O chemical shifts for several reduced POMs.

Computational Details

We used the ADF 2003.01 package[20] to compute the geometries of the molecules reported here. The density-functional theory (DFT) calculations are characterized by the local density approximation featuring the *Xa* model for exchange with Becke's gradient-corrected functional,[21] and the VWN parameterization for correlation[22] corrected

[a] Departament de Quimica Fisica i Inorgánica, Universitat Rovira i Virgili,
Marcel.lí Domingo s/n, Campus Sescelades, 43007 Tarragona, Spain
E-mail: josepmaria.poblet@urv.net
[b] Institute of Physical chemistry, Russian Academy of Sciences, 31, Leninski pr, Moscow 119991, Russia
E-mail: leoka@ipc.rssi.ru
[c] Department of Chemistry, State University of New York at Buffalo,
312 Natural Sciences Complex, Buffalo, NY 14260-3000, USA
Supporting information for this article is available on the WWW under http://www.eurjic.org or from the author.

with Perdew's functional.[23] The basis functions for describing the valence electrons of all the atoms are Slater-type orbitals of triple-ζ+ polarization quality. The internal or *core* electrons are described by means of single Slater functions and were generated with the auxiliary program DIRAC.[20] Quasi-relativistic corrections − *zeroth-order relativistic approximation* (ZORA) − were performed with corrected core potentials. The NMR shielding tensors were computed from a parallel version of the NMR module.[24]

The calculated chemical shift, δ_{cal}, is determined as the difference between total shielding of the reference molecule, σ_r, and the shielding, σ_x, of the molecule being studied:

$\delta_{cal} = \sigma_r - \sigma_x$

For each nucleus, the total shielding tensor, σ_t, is calculated as the sum of the paramagnetic (σ_p) and diamagnetic (σ_d) contributions. The simplest oxoanion, WO_4^{2-}, is usually used as a reference for ^{183}W NMR spectroscopy (calculated σ_t is 2663 ppm).[25] The ^{17}O NMR chemical shift is measured relative to pure water (δ = 0 ppm) for which the absolute shielding, σ_t, is 291 ppm.[26]

It is well known that when electrons are added to the structure the framework swells somewhat (i.e. some bonds are elongated).[15,27–30] Thus, in all cases, for both the parent oxidized POM and its reduced counterparts, the structures used were the optimized ones before and after the two electrons had been introduced.

Results and Discussion

$W_5O_{18}WNO^{3-}$

This anion is a derivative of the Lindqvist anion that contains one tungsten atom in the formal oxidation state 2+ with an NO group in place of the terminal oxygen atom. Formally, NO has a charge of 1+.[16] The oxidized anion has no counterpart and for purposes of comparison the Lindqvist anion is used. Although the X-ray geometry of this anion was not determined because the lattice cells are very similar, the atomic coordinates were inferred from the general description of the related anion $Mo_5O_{18}MoNO^{3-}$ and by comparison with the Lindqvist molybdate and tungstate anions. The symmetry of the anion is C_{4v}, which leads to three types of tungsten atoms (Figure 1). Three resonances are observed in the ^{183}W NMR spectrum with an intensity ratio of 1:4:1, the first of which is substantially shifted to low field (Table 1) and assigned to the reduced tungsten linked to NO. It should be noted that the experimental shift for W_c is markedly lower than the expected one for a $W(d^4)$ configuration. Due to the back-donation from tungsten to the nitrosyl group less electron density is left on tungsten, which results in a smaller chemical shift. The ^{183}W and ^{17}O NMR chemical shifts calculated for the optimized structure are given in Table 1.

The calculations correctly describe the pattern of the ^{183}W chemical shifts, although the value for W_c is considerably underestimated. The HOMO with *e* symmetry shows a π interaction between the W metal and the NO group (see Figure 1).

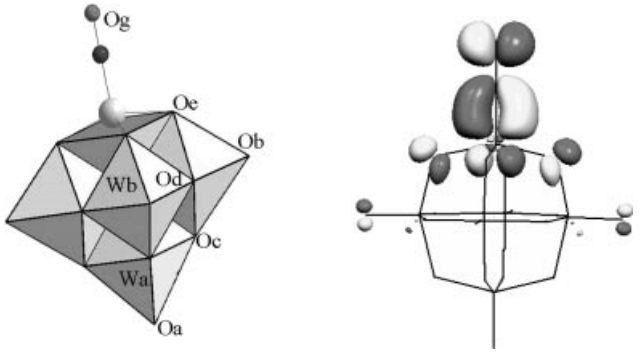

Figure 1. Structure and HOMO of $W_5O_{18}WNO^{3-}$.

Table 1. Calculated parameters and experimental ^{183}W and ^{17}O NMR shifts for $W_5O_{18}WNO^{3-}$.

	W_c	W_b	W_a	O_a	O_b	O_c	O_d	O_e	O_f
δ_{cal} [ppm]	488	225	197	699	717	456	438	517	–27
δ_{exp} [ppm]	653	168	117	728	734	402	399	448	

The ^{17}O NMR chemical shifts calculated for several oxygen atoms enable the lines observed for both the terminal and bridging (O_c and O_d, respectively) atoms to be assigned. It should be pointed out that the chemical shift for the bridging O_e is larger than for the other bridging atoms. This may be due to an interaction with the cation with the lowest oxidation state (W_c)[16] or the influence of the passing electron density. However, the oxygen atoms of this type have a higher shift[25] in $CH_3OTiW_5O_{18}^{3-}$, where no delocalization occurs. It should be noted that, as before, the chemical shifts calculated for the bridging oxygen atoms are overestimated and for the terminal ones they are underestimated.[25] Nevertheless, if compared with $W_6O_{19}^{2-}$, the computed ^{17}O chemical shifts correctly represent the marked decrease in the experimental shifts for all the oxygen atoms in $W_5O_{18}W_cNO^{3-}$.

γ-$SiW_{12}O_{40}^{n-}$

The structure of this anion, determined by Tézé et al.,[10] is the result of two triplet groups (W_a–W_b–W_b) rotated by 60° along two C_3 axes of the Keggin anion (Figure 2). This structure gives rise to four resonances with a 2:1:2:1 intensity pattern. The most shielded atoms in the ^{183}W NMR spectrum proved to be the W_a tungstens in rather a peculiar position (Table 2).[10]

According to the ^{183}W NMR spectrum, the two-electron-reduced form reveals an uneven distribution of the electron density over the coordination sphere. The most deshielded atoms proved to be W_d, which acquire the largest portion of the electron density, and the least shielded are W_c. Experimentally, the assignment of the resonance lines for the reduced species is ambiguous because the quality of the spectrum did not allow the spin–spin coupling to be determined. However, the present calculations unambiguously show that W_d is reduced first because the LUMO that acquires two electrons mainly consists of W_d d_{xy} orbitals and,

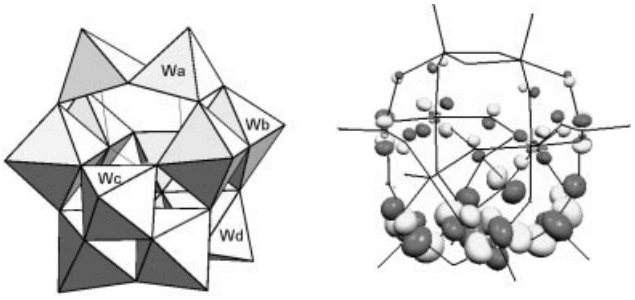

Figure 2. Structure and HOMO of the two-electron-reduced γ-$SiW_{12}O_{40}^{6-}$.

Table 2. Calculated and experimental ^{183}W NMR chemical shifts [ppm] for the oxidized γ-$SiW_{12}O_{40}^{4-}$ and 2e-reduced γ-$SiW_{12}O_{40}^{6-}$ anions.

	W_a	W_b	W_c	W_d
$\delta^{ox}{}_{exp}$[a]	–160	–105	–117	–127
$\delta^{ox}{}_{cal}$[b]	–170	–130	–184	–158
$\delta^{red}{}_{exp}$[a]	–131	–63	–124	489
$\delta^{red}{}_{cal}$[b]	–47	–2	–65	471
$\delta^{*}{}_{cal}$[c]	–63	–63	–98	–32
$\Delta\delta_{geom}$[d]	+107	+67	+86	+126
$\Delta\delta_{elect}$[d]	+16	+61	+33	+503

[a] Observed NMR chemical shifts for the fully oxidized ($\delta^{ox}{}_{exp}$) and 2e-reduced ($\delta^{red}{}_{exp}$) anions. [b] Computed NMR chemical shifts for the fully oxidized ($\delta^{ox}{}_{cal}$) and 2e-reduced ($\delta^{red}{}_{cal}$) anions in their optimal structures. [c] $\delta^{*}{}_{cal}$ is the shift computed for the oxidized anion but with the structure of the reduced anion. [d] $\Delta\delta_{geom} = \delta^{*}{}_{cal} - \delta^{ox}{}_{calc}$ represents the shift induced by the geometrical change and $\Delta\delta_{elect} = \delta^{red}{}_{cal} - \delta^{*}{}_{calc}$ the shift resulting from the incorporation of the electron density in the already deformed anion (see text for more details).

to a lesser extent, W_b tungsten atoms; W_a and W_c are reduced afterwards. Nevertheless, in the observed spectrum of the reduced anion one of the resonance lines (δ = –131 ppm) is negatively shifted with respect to the lines of the oxidized anion. The notable positive calculated shifts (>100 ppm) of the lines assigned to W_a and W_c for the reduced anion will be discussed below.

It should also be noted that, despite an increase in the electron population on the reduced tungsten, the diamagnetic shielding does not differ much (δ = 5 ppm) from the diamagnetic shielding for nonreduced tungstens.

$P_2W_{18}O_{62}^{6-}$

This is the largest anion considered in this paper (Figure 3). Its ^{183}W NMR spectrum completely corresponds to the two expected resonance lines with an intensity ratio of 1:2, the first of which is assigned to the cap tungsten atoms (W_a) (Table 3).[9] It should be noted that W_b is linked to other tungsten atoms with three corner- and one edge-shared oxygen atoms, unlike W_a, which is linked by two corner- and two edge-shared oxygen atoms as in the Keggin anion.

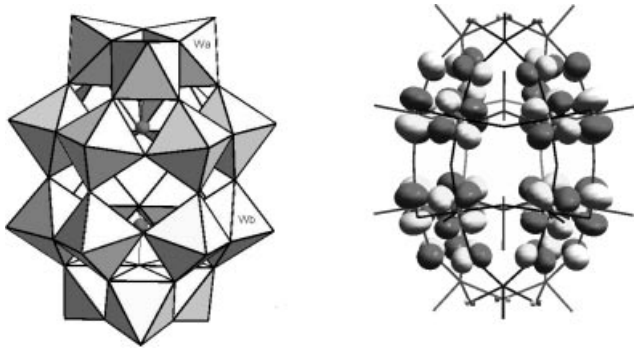

Figure 3. Structure and HOMO of the two-electron-reduced $P_2W_{18}O_{62}^{8-}$.

Table 3. Calculated and observed ^{183}W NMR chemical shifts [ppm] for the oxidized $P_2W_{18}O_{62}^{6-}$ and 2e-reduced $P_2W_{18}O_{62}^{8-}$ anions.[a]

	W_a	W_b
$\delta^{ox}{}_{exp}$	–127	–173
$\delta^{ox}{}_{cal}$	–146	–215
$\delta^{red}{}_{exp}$	–299	–51
$\delta^{red}{}_{cal}$	–193	–143
$\delta^{*}{}_{cal}$	–105	–134
$\Delta\delta_{geom}$	41	81
$\Delta\delta_{elect}$	–88	–9

[a] See Table 2 for definitions of the chemical shifts.

Reducing the anion with two electrons completely delocalizes the electron pair over 12 W_b atoms. As shown by different calculation approaches, the HOMO (Figure 3), which contains two electrons, is composed of symmetry-adapted W^5 d_{xy} orbitals of the belt tungsten atoms W_b. This is clear from the marked positive shift of the more intense resonance line. At the same time, the resonance assigned to the cap tungsten atoms W_a undergoes a substantial negative shift.

Despite the notable discrepancy between the calculated and experimental chemical shifts, and although the calculated absolute shifts upon reduction are markedly less than the observed ones (Table 3), the DFT calculation adequately reflects how the chemical shifts tend to change upon reduction.

$W_{10}O_{32}^{4-}$

Like the Dawson anion $P_2W_{18}O_{62}^{6-}$ considered above, this decatungstate may be viewed as a combination of two fragments of the initial anion, in this case the Lindqvist anion (Figure 4). $W_{10}O_{32}^{4-}$ also gives two resonance lines in the ^{183}W NMR spectrum at δ = –23 and –165 ppm, with an intensity ratio of 4:1, both of which are shifted to high field with respect to the parent anion (δ = +59 ppm).[11] In contrast to the Dawson anion, two-electron reduction of $W_{10}O_{32}^{4-}$ induces positive shifts in both resonances. However, the second line shifts by only 16 ppm, while the first one shifts by 330 ppm, strongly indicating that the electron pair is delocalized over eight tungsten atoms of the W_b type.

This is also confirmed by the nature of the HOMO, which consists of symmetry-adapted d_{xy} orbitals of W_b (Figure 4).

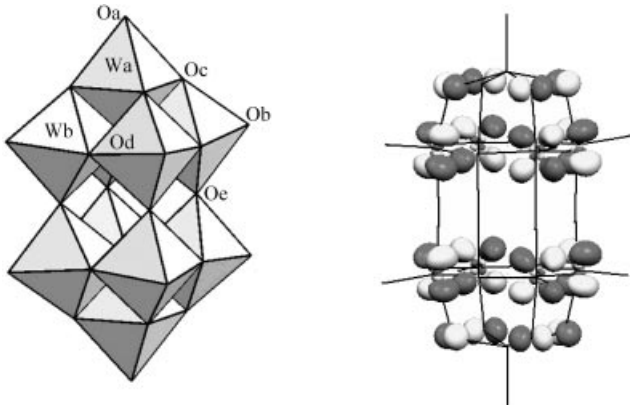

Figure 4. Structure and HOMO of the two-electron-reduced $W_{10}O_{32}^{6-}$.

A slight positive shift in the line assigned to W_a might indicate the delocalization of electron density on these atoms, as was observed in γ-$SiW_{12}O_{40}^{6-}$. However, this may be misleading. We should bear in mind that when an anion is reduced, it "swells" because the bond lengths increase. According to the X-ray structure determination of the oxidized and reduced species[30] of the decatungstate, both types of WO_6 octahedron increase in size slightly, which is confirmed by the structures computed for oxidized and reduced anions. The geometry changes most in the belt octahedra (see the bond lengths in Table 4).

Table 4. Observed and calculated NMR shieldings for $W_{10}O_{32}^{n-}$.[a]

	W_a	W_b	O_a	O_b	O_c	O_d	O_e	O_f
$W_{10}O_{32}^{4-}$								
R_{WO} [Å]	1.966	1.983	1.756	1.739	1.938/ 1.969	1.942	1.923	2.288/ 2.354
δ^{ox}_{exp} [ppm]	–165	–23	732	765	434	421	423	–1.6
δ^{ox}_{cal} [ppm]	–155	–41	707	751	494	485	471	–49
δ^{*}_{cal} [ppm]	–39	109	733	784	524	505	480	–58
$\Delta\delta_{geo}$ [ppm]	+116	+150	+26	+33	+30	+20	+9	–9
$W_{10}O_{32}^{6-}$								
R_{WO} [Å]	1.978	1.994	1.789	1.762	1.939/ 2.024	1.942	1.928	2.325/ 2.365
δ^{red}_{exp} [ppm]	–149	307	662	709	349	405	419	–2.4
δ^{red}_{cal} [ppm]	–58	249	632	693	412	465	479	–50
$\Delta\delta_{elect}$ [ppm]	–19	+140	–101	–91	–112	–40	–1	+8

[a] See Table 2 for definitions of the chemical shifts.

The calculated charge on the W_b atoms decreases upon reduction, and there is practically no change in W_a.[31] In other words, the positive shift for W_a is caused by a geometrical change in the cap octahedron due to the reduction of the vicinal tungstens.

Unlike in the ^{183}W NMR spectrum, all the ^{17}O NMR resonances shift to high field upon reduction. These negative shifts may be the result of the delocalization of the electron density, the shielding of the nuclei, or the exclusion of the HOMO (LUMO before reduction) from the transitions that determine the paramagnetic term. From the calculated charges, only the O_c atoms seem to reveal some increase in their negative charge upon reduction. Thus, the substantial negative shifts may be assumed to be due to an increase in the paramagnetic shielding. It should be noted that the ^{17}O resonance line assigned to the O_e linking two fragments undergoes the least negative shift, despite delocalization of the electron pair over W_b. Once again, if the shifts calculated for $W_{10}O_{32}^{4-}$ and $W_{10}O_{32}^{6-}$ are compared using the geometry for the reduced anion, we see that the decrease in the shifts is larger.

It should be noted that despite localization of the electron density over the eight W_b atoms, the terminal oxygen atom W_a feels the presence of the electron pair in the HOMO, which is probably excluded from the principle transitions that determine the paramagnetic shielding. On the other hand, O_e does not react to the presence of the electron density on the nearest W_b tungsten atoms. Presumably because of selection rules, the HOMO does not participate in the transitions that determine the paramagnetic contribution of these oxygen atoms.

Electronic and geometric factors also influence the calculated chemical shifts. For example, the reduction of a tungsten ion *always* induces a positive shift in the ^{183}W NMR resonance in polytungstates. The present DFT calculations reproduce this phenomenon fairly well and show that the greater the electron density on a given nucleus the greater the chemical shift. It increases from the Dawson anion (2 e per 12 W_b), to decatungstate (2 e per 8 W_b), and then to the γ-Keggin anion (2 e per 4 W_d and partially on another 4 W_b).

The incorporation of one electron into a nonbonding metal orbital is associated with a small enlargement in the reduced octahedron. By analyzing the chemical shift in several geometries we managed to separate the electronic factors from the geometric factors causing this positive shift. For some of the anions discussed above we calculated the chemical shifts for the oxidized parent anions but using the optimized geometry for the reduced form. In all cases, substantial positive shifts of the calculated values δ^{*}_{cal} were found, therefore $\Delta\delta_{geom}$ ($\delta^{*}_{cal} - \delta^{ox}_{cal}$) will be considered as the geometry factor due to the enlargement of the anion as a result of reduction. On the other hand, the shift due to incorporation of the electron density, $\Delta\delta_{elec}$, is given by $\delta^{red}_{cal} - \delta^{*}_{cal}$, where calculated values refer to the optimized structure of the reduced form. The importance of the electronic effect increases as the charge density on the reduced center increases. Hence, in the γ-$SiW_{12}O_{40}^{6-}$ anion the electronic term for W_d was estimated to be four times larger than the geometric term. For W_b in $W_{10}O_{32}^{6-}$ the two terms are of similar weight. The electronic effect must be much less important in the case of the Dawson anion, where the two extra electrons are shared by 12 centers, therefore the positive shift is due to enlargement of the anion (see Table 3).

We will now discuss the case of $W_{10}O_{32}^{4-}$ in some detail. The 2e-reduction shifts the signal associated to the reduced belt tungstens (W_b) by +330 ppm. The corresponding computed value is +290 ppm. By calculating the chemical shift of the oxidized anion with the geometry of the reduced

partner, we estimate that the geometrical effect is +150 ppm ($\Delta\delta_{geo}$). Thus, the addition of two electrons to the already adapted (enlarged) framework shifts the signal by a further +140 ppm ($\Delta\delta_{elec}$). For the nonreduced W_a, the calculated shift is +97 ppm, a very high value in comparison with the experimental value of +16 ppm. The DFT calculations probably overestimate the deformation of the cap octahedra ($\Delta\delta_{geo}$ = +116 ppm) due to the reduction of a belt site.

As mentioned above, the two added electrons in γ-$SiW_{12}O_{40}^{6-}$ are shared mainly by four tungstens. Consequently, the electronic term is much more important. $\Delta\delta_{elec}$ for W_d was computed to be +503 ppm, whereas the corresponding $\Delta\delta_{geo}$ contribution is only +126 ppm. As for $W_{10}O_{32}^{4-}$, the relatively large $\Delta\delta_{geo}$ values for the nonreduced centers seem to be the cause of their large positive shift.

Figure 5 compares the calculated and experimental ^{183}W chemical shifts for the reduced and parent anions, and gives important data for $W_5O_{18}W_cNO^{3-}$. From the position of the points, it can be assumed that the values calculated for the reduced anions are slightly overestimated, because the linear trend seems to be positively shifted. This shows that the increase in the chemical shifts is not only due to the reduction but also because the additional electrons lead to an enlargement of the structure. The positive shift of 65 ppm of the trend may assume that the optimization of the structure in the reduced state slightly overestimates the bond lengths.

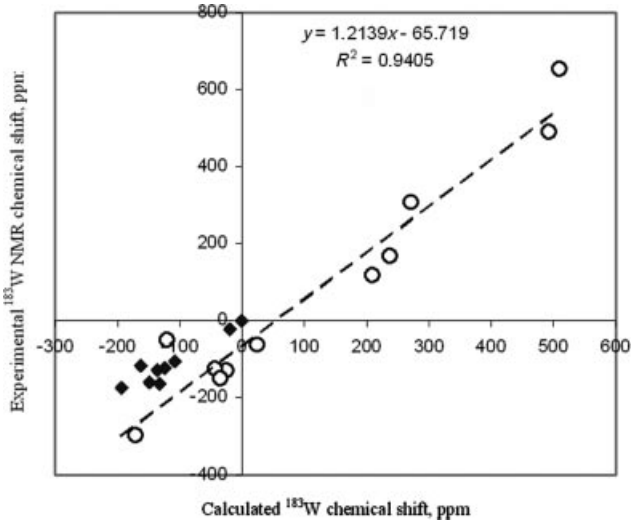

Figure 5. Correlation of the experimental and calculated ^{183}W chemical shifts for reduced and parent anions: ♦ oxidized anions, o reduced anions.

Analysis of the transitions responsible for the paramagnetic shielding of different tungsten atoms may clarify the situation for those atoms for which the resonances with less-positive shifts are assigned.

Conclusions

DFT calculations have been carried out to analyze the effect of reduction on the ^{183}W and ^{17}O chemical shifts in several prototypic polyoxotungstates. In general, the experimental trends are well reproduced, although significant discrepancies were found between some computed and observed values. This deviation is especially important for the W^{II} ion in the Lindqvist derivative $W_5O_{18}W^{II}NO^{3-}$, probably due to the inability of DFT methods to properly describe the interaction between the W^{II} ion and the NO ligand.

The incorporation of one electron in a nonbonding metal orbital produces an enlargement of the reduced octahedron. By analyzing the chemical shift in several geometries we have been able to separate the electronic factors from the geometric factors that cause the positive shift. The importance of the electronic effect increases with the charge density on the reduced center, hence in the γ-$SiW_{12}O_{40}^{6-}$ anion the electronic term has been estimated to be three times larger than the geometric term, whereas for $W_{10}O_{32}^{6-}$ the two terms have similar weight. The electronic effect must be much less relevant in the Dawson anion, where the two extra electrons are shared by 12 centers. This means that the small positive shift should be mainly attributed to a change in the geometry as a consequence of the reduction. The present calculations have not allowed us to rationalize the extremely negative shift of the resonance line assigned to the cap W_a in reduced $P_2W_{18}O_{62}^{8-}$.

The ^{17}O NMR lines are negatively shifted upon reduction, in contrast to the positive shifts resulting from placing the electron density on the tungsten atoms. The large negative shift of the resonance of O_a in $W_{10}O_{32}^{6-}$, which is rather far away from the delocalized electron pair, is especially surprising. Further analysis of the calculated ^{17}O NMR chemical shifts may clarify this situation.

Supporting Information (see footnote on the first page of this article): Decomposition of shielding tensors into their paramagnetic and diamagnetic contributions is given as Supporting Information (Tables S1–S4).

Acknowledgments

This work was supported by the Spanish MECD (BQU2002-04110-C02-01) and the CIRIT of the Autonomous Government of Catalonia (SGR01-00315). J.A. is grateful for financial support from the CAREER program of the National Science Foundation (grant no. CHE-0447321). The authors thank the referees for comments and suggestions.

[1] M. T. Pope, *Heteropoly and Isopoly Oxometalates*, Springer, Berlin, **1983**.
[2] a) *Polyoxometalates: From Platonic Solids to Anti-Retroviral Activity* (Eds.: M. T. Pope, A. Müller), Kluwer, Dordrecht, **1994**; b) M. T. Pope, A. Müller, *Angew. Chem. Int. Ed. Engl.* **1991**, *30*, 34–48.
[3] *Chem. Rev.* **1998**, *98*, 3 special issue, Ed.: C. Hill.
[4] *Polyoxometalates* (Eds.: J. J. Borrás-Almenar, E.Coronado, M. T. Müller, A. Pope), Molecular Science NATO Science Series. II, Mathematics, Physics and Chemistry, **2003**, vol. 98, Kluwer Academic Publishers, Dordrecht.
[5] C. Sanchez, J. Livage, J. P. Launay, M. Fournier, Y. Jeannin, *J. Am. Chem. Soc.* **1982**, *104*, 3194.
[6] C. Sanchez, J. Livage, J. P. Launay, M. Fournier, *J. Am. Chem. Soc.* **1983**, *105*, 6817.

[7] K. Piepgrass, J. N. Barrows, M. T. Pope, *J. Chem. Soc., Chem. Commun.* **1989**, 10.
[8] P. Kazansky, M. A. Fedotov, I. V. Potapova, V. I. Spitsyn, *Dokl. Akad. Nauk.* **1979**, *244*, 372.
[9] K. Kozik, C. F. Hammer, L. C. W. Baker, *J. Am. Chem. Soc.* **1986**, *108*, 2748.
[10] a) A. Tézé, J. Canny, L. Gurban, R. Thouvenot, G. Hervé, *Inorg. Chem.* **1996**, *35*, 1001; b) A. Tezé, E. Cadot, V. Béreau, G. Hervé, *Inorg. Chem.* **2001**, *40*, 2000.
[11] D. C. Duncan, C. L. Hill, *Inorg. Chem.* **1996**, *35*, 5828.
[12] E. Cadot, V. Bereau, B. Marg, S. Halut, F. Secheresse, *Inorg. Chem.* **1996**, *35*, 3099.
[13] K. Kozik, L. C. W. Baker, in *Polyoxometalates* (Eds.: M. T. Pope, A. Muller), Kluwer Academic Publishers, **1994**, p. 191.
[14] K. Piepgrass, M. T. Pope, *J. Am. Chem. Soc.* **1987**, *109*, 1586.
[15] T. Yamase, E. Ishikawa, *J. Chem. Soc., Dalton Trans.* **1996**, 1619.
[16] A. Proust, R. Thouvenot, S. G. Roh, J. K. Yoo, P. Gouzerh, *Inorg. Chem.* **1995**, *34*, 4106.
[17] A. Proust, M. Fournier, R. Thouvenot, P. Gouzerh, *Inorg. Chim. Acta* **1994**, *215*, 61.
[18] C. Rong, M. T. Pope, *J. Am. Chem. Soc.* **1992**, *114*, 293–298.
[19] A. Bagno, M. Bonchio, A. Sartorel, G. Scorano, *Eur. J. Inorg. Chem.* **2000**, 17.
[20] a) ADF 2003.01, Department of Theoretical Chemistry, Vrije Universiteit, Amsterdam; b) E. J. Baerends, D. E. Ellis, P. Ros, *Chem. Phys.* **1973**, *2*, 41; c) L. Versluis, T. Ziegler, *J. Chem. Phys.* **1988**, *88*, 322; d) G. Te Velde, E. J. Baerends, *J. Comput. Phys.* **1992**, *99*, 84; e) C. Fonseca Guerra, J. G. Snijders, G. Te Velde, E. J. Baerends, *Theor. Chem. Acc.* **1998**, *99*, 391.
[21] A. D. Becke, *J. Chem. Phys.* **1986**, *84*, 4524; A. D. Becke, *Phys. Rev. A* **1988**, *38*, 3098.
[22] S. H. Vosko, L. Wilk, M. Nusair, *Can. J. Phys.* **1980**, *58*, 1200.
[23] J. P. Perdew, *Phys. Rev. B* **1986**, *33*, 8822; J. P. Perdew, *Phys. Rev. B* **1986**, *34*, 7406.
[24] J. Autschbach, E. Zurek, *J. Phys. Chem. A* **2003**, *107*, 4967–4972.
[25] J. Gracia, J. M. Poblet, J. Autschbach, L. P. Kazansky, *Eur. J. Inorg. Chem.* **2006**, 1139–1148; preceding article.
[26] D. Sundholm, J. Gauss, A. Schäfer, *J. Chem. Phys.* **1996**, *105*, 11051.
[27] J. N. Barrows, G. B. Jameson, M. T. Pope, *J. Am. Chem. Soc.* **1985**, *107*, 1771.
[28] R. Neir, C. Trojanovski, R. Mattes, *J. Chem. Soc., Dalton Trans.* **1995**, 2521.
[29] E. Ishikawa, T. Yamase, *Bull. Chem. Soc. Jpn.* **2000**, *73*, 641.
[30] Y. Sasaki, T. Yamase, Y. Ohashi, Y. Sasada, *Bull. Chem. Soc. Jpn.* **1987**, *60*, 4285.
[31] L. P. Kazansky, T. Yamase, *J. Phys. Chem. A* **2004**, *108*, 6437.

Received: September 19, 2005
Published Online: February 6, 2006

